IPPP/23/43
LTH-1349

Dark Matter (H)eats Young Planets

Djuna Croon[1,*] and Juri Smirnov[2,†]

[1] Institute for Particle Physics Phenomenology, Department of Physics, Durham University, Durham DH1 3LE, U.K.
[2] Department of Mathematical Sciences, University of Liverpool, Liverpool, L69 7ZL, United Kingdom

(Dated: September 7, 2023)

We study the effect of dark matter annihilation on the formation of Jovian planets. We show that dark matter heat injections can slow or halt Kelvin-Helmholtz contraction, preventing the accretion of hydrogen and helium onto the solid core. The existence of Jupiter in our solar system can therefore be used to infer constraints on dark matter with relatively strong interaction cross sections. In the case of spin-dependent dark matter, we derive novel constraints beyond the reach of current direct detection experiments. We highlight the possibility of a positive detection using future observations by JWST, which could reveal strongly varying planet morpholoiges close to our Galactic Center.

Our technical capabilities to detect planets outside our solar system have developed dramatically. From the first indirect evidence for an exoplanet [1], to direct imaging [2] and precision atmospheric observations [3], we have now 5.5×10^3 detected exoplanets, and $\mathcal{O}(10^4)$ candidates awaiting confirmation [4]. With the onset of high performance infra-red astronomy and the JWST [5], and Roman [6] space missions low temperature targets, such as exoplanets can be studied across the galaxy, all the way to the Galactic Center (GC). This development opens up a new window to our galaxy, and allows us to study exoplanets in various astrophysical environments.

Dark Matter (DM) as the dominant mass source in our galaxy is well mapped by stellar kinematics, and despite uncertainties displays a density profile that raises towards the GC [7]. In the search for this ellusive substance a number of studies have considered DM capture in celestial object ranging from solar system objects such as the Earth, Sun [8–30], Jupiter [8, 31–34], and Uranus [35], to Brown Dwarfs [36, 37], White Dwarfs [38], Neutron Stars [37, 39–76], and other stars [77–83], as well as recently Exoplanets [36, 84]. For a recent review of searches in compact stars, see [85]. Many of the above studies rely on an energy injection from DM particles that annihilate after being captured by the celestial object. This is expected in models where DM has been thermally produced in the early universe.

Jovian exoplanets have been identified as ideal candidates for DM capture in Ref. [36]. The advantage is their relatively large surface gravity, combined with rather low core temperatures, leading to DM with low masses to be retained in the object. Their hydrogen-rich composition makes them kinematically well suited for capturing DM particles around the GeV scale, and especially particles with spin-dependent nuclear interactions. The differential measurement of Jovian planet and Brown Dwarf temperatures close to the GC has been identified as a promising tool to detect heating from annihilating DM [36].

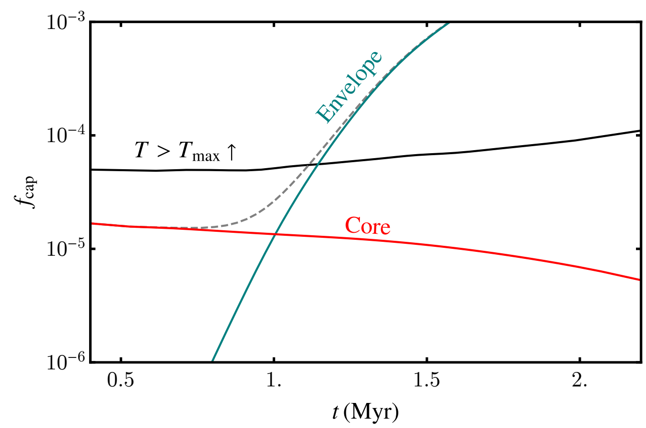

FIG. 1. Captured DM fraction in a benchmark scenario for spin-dependent dark matter: $m_{\rm DM} = 5$ GeV, $\sigma_p = 10^{-27}$ cm^2. Dark matter density and velocity as in the solar system. The red line gives the fraction of the dark matter flux through the planet that is captured by the core, the cyan line gives the fraction captured by the envelope, and the dashed line the total captured fraction. Above the black line labeled $T > T_{\rm max}$ dark matter annihilation heats the planet above the temperature defined by Eq. (2), which halts the formation process.

In this work we propose a more radical possibility. By investigating the formation process of Jovian planets we argue that an additional heat source associated with DM annihilation could halt the formation process at various stages, depending on the DM parameters, such as mass, cross section, and ambient number density. Thus, we would expect to have varying properties of Jovian planets across the galaxy, or their total absence under certain circumstances.

The mere existence of Jupiter in our solar system allows us to set new constraints on the parameter space of DM, which are especially competitive in the case of spin-dependent interactions. We find that future observations of exoplanets near the GC, enabled by the JWST and future infrared telescopes will further test yet unconstrained parameter space of DM candidates across a wide range of masses and interaction cross sections.

* djuna.l.croon@durham.ac.uk; ORCID: 0000-0003-3359-3706
† juri.smirnov@liverpool.ac.uk; ORCID: 0000-0002-3082-0929

Planet formation – We focus on giant, Jovian planets, and the formation process called core-accretion gas-capture [86], which proceeds in two stages. First, a solid core made of heavier elements, such as ice and silica forms within a fraction of a Myr. These planets form beyond the frost line of a solar system, where icy compounds are cool enough to remain solid, allowing cores to become heavy enough to start to accrete hydrogen and helium. Planets formed closer to their sun, such as Earth, on the inside the frost line have cores dominated by iron and silicates, which are too rare to lead to large cores that would accrete gas.

Gas capture does not begin until the core accretion exceeds about $10M_\oplus$ ($M_\oplus = 6.0 \times 10^{24}$ kg), when the growing core raises the escape velocity above the thermal velocity of the nebular gas. The proto-planet then accumulates a gas envelope at an increasing rate, reflecting its increasing mass. The gas can quickly fill up the Bondi sphere of the planet, which subsequently needs to cool via the Kelvin-Helmholtz mechanism in order to accrete further [87]. Therefore, during the gas accretion period (which takes place on the scale of a Myr [88]) the system remains in a quasi-equilibirum state where gas accretion can only proceed once the excess heat that is released from the gravitational binding energy has been radiated away. It is then not surprising that an additional heat source can disrupt this fragile equilibrium and lead to drastically different outcomes. Note in particular that the hydrogen accretion stage is unique, as hydrogen atoms have the lowest gravitational binding energy and are thus most susceptible to evaporation from the forming planet.

Disrupting Jovian Formation – We assume that DM is produced in a scenario resulting in equal abundances of DM particles and antiparticles. In the presence of elastic scattering interactions with standard model (SM) particles, DM can scatter in forming planets, lose its kinetic energy, and become gravitationally captured. Once its number density is large enough for particle-anti-particle annihilation to become efficient, it can become an additional substantial heat source in the system. Thus, it may slow or halt Kelvin-Helmholtz contraction, in turn preventing the accretion of gas and the formation of Jovian planets. The effect becomes relevant once the energy injection due to DM annihilation is comparable to the power generated by the Kelvin-Helmholtz mechanism.

Contraction is set by the net energy loss, which is modified in the presence of DM annihilation,

$$\begin{aligned} \dot{Q} - L_{\rm DM}(R) &= -\frac{dU}{dt} \\ 4\pi R^2 \times \sigma_{\rm SB} T^4 - L_{\rm DM}(R) &= c_1 \frac{GM^2}{R^2}\frac{dR}{dt} \end{aligned} \tag{1}$$

where $\dot{Q}$ is the radiative heat loss, dU/dt the change in gravitational potential energy, $L_{\rm DM}(R)$ is the R dependent heat injection due to DM annihilation, which we call DM luminosity, and $1/2 \leq c_1 \leq \infty$ is a factor which depends on the internal mass distribution (for a uniform sphere, $c_1 = 3/5$).

Initially, dark matter heat injections will raise the temperature of the protoplanet, increasing its radiative heat loss. However, above a certain temperature the mixture of hydrogen and helium gas acquires enough thermal energy such that particles near its surface reach the escape velocity. We estimate that this happens for temperatures above which

$$\Gamma_{\rm J}(T) = \frac{nv}{2\sqrt{\pi}}\left(1 + \frac{v_{\rm esc}^2}{v^2}\right)\exp\left(-\frac{v_{\rm esc}^2}{v^2}\right)\Bigg|_{T=T_{\rm max}} = C\dot{M} \tag{2}$$

where $\Gamma_{\rm J}$ is the flux of escaping particles given by the Jeans escape formula [89], with n the number density of gas particles, $v_{\rm esc}$ the surface escape velocity, $v = \sqrt{2T/m}$, with m being the mass of the gas particle, and $\dot{M}$ is the rate of growth of the planet in the absence of dark matter heat, which we take from simulation results presented in [90, 91]. Equation (2) overestimates the actual loss rate because it assumes the tail of the velocity distribution is replenished instantaneously, Therefore, to be conservative, we take $C = 10$. This gives us maximum hydrogen escape temperatures of $T_{\rm max} \sim 8$ K and 10^3 K in the envelope and in the core respectively.

Thus, the maximum heat loss happens just below $T_{\rm max}$ and we estimate that DM heat injection halts collapse if

$$\begin{aligned} L_{\rm DM} &\geq 4\pi R^2 \sigma T_{\rm max}^4 \\ &\geq 4 \times 10^{-8} \times \left(\frac{R}{10^3 R_p}\right)^2 \left(\frac{T_{\rm max}}{8\rm K}\right)^4 \rm L_\odot \end{aligned} \tag{3}$$

where $R_p = 7 \times 10^5$ km is the radius of Jupiter (the protoplenatary envelope has radius $\sim 10^3 R_p$), and where $L_\odot = 2 \times 10^{36}\,\rm GeV\,s^{-1}$ is the luminosity of the Sun. To investigate whether Eq. (3) is satisfied in the evolution of the planet, we use the simulation results presented in [91]. We will now examine how the DM luminosity depends on the properties of the capturing object, and the DM particle model.

Dark matter energy injection – To obtain the DM luminosity, we assume DM annihilation equilibrium – motivated a posteriori below – i.e. that each incoming DM particle that is captured contributes its rest mass immediately to the energy budget. We will discuss why this treatment is justified in the following subsection. We thus can write

$$L_{\rm DM} = m_\chi C_{\rm cap} = m_\chi f_{\rm cap}\Phi \tag{4}$$

where m_χ is the DM mass, $C_{\rm cap}$ is the capture rate, and $f_{\rm cap}$ the captured fraction of the DM flux Φ passing through the object, given by

$$\Phi = v_{\rm DM}\sqrt{\frac{8}{3\pi}}\frac{\rho_{\rm DM}}{m_\chi}\left(1 + \frac{3}{2}\frac{v_{\rm esc}^2}{v_{\rm DM}^2}\right). \tag{5}$$

Then, we have

$$L_{\rm DM} \sim 2\times 10^{-9} f_{\rm cap} \left(\frac{R}{10^3 R_p}\right)\left(\frac{M}{10 M_\oplus}\right) \times \left(\frac{v_{\rm DM}}{270 {\rm km\,s^{-1}}}\right)^{-1}\left(\frac{\rho_{\rm DM}}{0.42\,{\rm GeV\,cm^{-3}}}\right) L_\odot \quad (6)$$

independently of the dark matter mass. It is seen that this may exceed (3) for greater M or $\rho_{\rm DM}$.

Dark matter capture – Given a certain DM mass and velocity, the DM particle needs a certain number of scatterings to drop below the escape velocity of a given object. This will in general also depend on the efficiency of the energy loss, determined by the mass ratio of the DM particle and the target nucleus. Furthermore, in the case of DM particles with masses similar of below the target mass, DM particles might be reflected off the object before capture can occur, as discussed in detail in Ref. [92, 93]. To compute the fraction of the DM particles that are captured in a given object we use the `Asteria` [92, 93] package, which takes all the above mentioned phenomena into account.

In this work we focus on DM interaction with nuclei and distinguish two broad DM model classes. The first is a model where the DM particle scatters with SM particles independently of their spin. Given an input DM nucleon cross section $\sigma_{\chi N}$, this leads to the spin-independent DM-nucleus cross section with an atomic number A nucleus

$$\sigma_{\rm SI} = \sigma^{\rm SI}_{\chi N} A^2 \left(\frac{\mu(m_\chi, m_A)}{\mu(m_\chi, m_N)}\right)^2, \quad (7)$$

where $\mu(m_\chi, m_{\rm SM})$ is the reduced mass of a DM and a SM particle of mass $m_{\rm SM}$. Note that it has been pointed out that at cross sections $\sigma_{\chi N} > 10^{-26}{\rm cm}^2$ the scattering is not described by interactions of point like particles, and the coherent scattering picture breaks down [94, 95]. Rather, at cross sections larger than this threshold the interaction can be assumed as a total geometric scattering cross section with the entire nucleus without an implied scaling with atomic number.

The second case of interactions we consider is a spin-dependent scattering cross section

$$\sigma_{SD} = \sigma^{\rm SD}_{\chi N} \frac{4\,(J_A+1)}{3 J_A}[a_p\langle S_p\rangle + a_n\langle S_n\rangle]^2 \left(\frac{\mu(m_\chi, m_A)}{\mu(m_\chi, m_N)}\right)^2, \quad (8)$$

where J_A is the nuclear spin of the target, $\langle S_p\rangle$ the average proton and $\langle S_n\rangle$ the average neutron spin of the nucleus. The a_p, and a_n are the DM model parameters indicating the coupling strength to protons and neutrons respectively. For example in the case of $a_p = 1$, and $a_n = 0$, the hydrogen scattering cross section is equal to the DM scattering cross section on protons $\sigma_{SD} = \sigma_p$, which we will use as a benchmark model.

We model the protoplanet in a simplified manner assuming that it consists of an icy core are an outer gas envelope, both are assumed to have a homogeneous average density. We use the mass and radius from Ref. [90] as time dependent input quantities. The outer envelope has a large radius and a low density. We model the envelope to consist of 75% hydrogen and 25% helium and compute the fraction of dark matter that is captured. We find that only at substantial cross sections above $10^{-28}{\rm cm}^2$ a substantial fraction of the DM particles are captured. The most efficient capture rate takes place in the GeV mass range, when the DM mass matches the hydrogen target mass. The core of the protoplanet is much more dense, which has the potential to increase the DM capture rate. We model the core as having a 58/42 ice (H_2O) to silica (SiO_2) mass ratio [88], which makes Oxygen the most abundant element. This implies that optimal capture happens for slightly heavier DM candidates, due to more efficient energy transfer between the SM and DM particles of similar mass.

TABLE I. Isotope fractions, nuclear spins, average proton, and neutron spins of the dominant isotopes considered.

Isotopes	**^{17}O**	**^{29}Si**	**^{1}H**
Abundance [%]	~ 0.4	~ 4.7	~ 100
J	5/2	1/2	1/2
$\langle S_p\rangle$	-0.036	0.054	0.5
$\langle S_n\rangle$	0.508	0.204	0

For the spin-dependent calculation, we need to estimate the mass fraction which is relevant for spin-dependent scattering. Thus we take the isotope fractions and properties of the elements in Tab. I.

Lastly, we note that light DM candidates can be reflected, such that the capture efficiency remains below one even at large cross sections [92]. As we will see below, this has implications for the sensitivity to subfractions of DM.

Dark matter annihilation – Neglecting DM evaporation from the celestial body, the Boltzmann equation governing the accumulation of DM is given by

$$\frac{dN}{dt} = C_{\rm cap} - C_{\rm ann} N_\chi^2, \quad (9)$$

where $C_{\rm cap}$ is the total capture rate of DM particles per unit time in the celestial object, and $C_{\rm ann} = \langle\sigma_{\rm ann} v\rangle / V_{\rm eff}$ the DM annihilation rate per effective volume, which is given by $1/V_{\rm eff} = \int_V n_\chi^2 / \int_V n_\chi$. After a characteristic time τ the system reaches annihilation equilibrium where $dN_\chi/dt \to 0$, which implies that $N_\chi \to \sqrt{C_{\rm cap}/C_{\rm ann}}$, leading to $\tau = 1/\sqrt{C_{\rm cap} C_{\rm ann}}$.

For our forming protoplanet the $V_{\rm eff} \approx V_{\rm core}$, which typically has a $R \sim 3\,R_\oplus$, we thus have

$$\tau \approx \sqrt{\frac{m_\chi\, 10^{-30}\ {\rm cm}^3/{\rm s}}{\langle\sigma_{\rm ann} v\rangle\ {\rm GeV}}}\ {\rm Myr}, \quad (10)$$

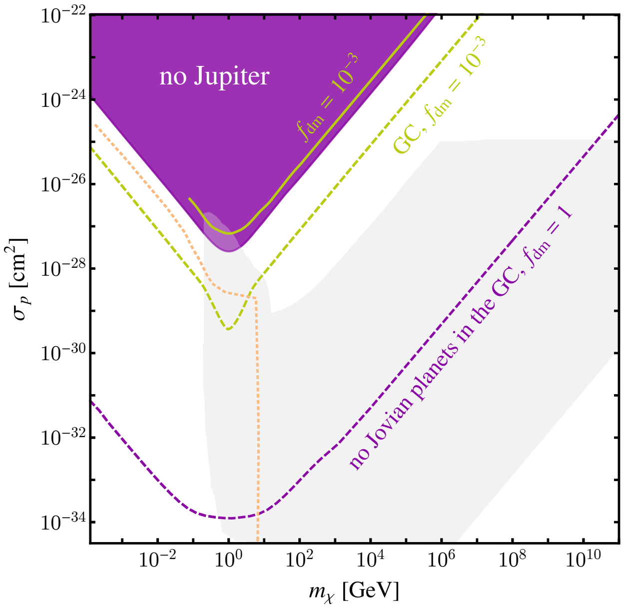

FIG. 2. Constraints on spin-dependent parameter space. The filled contour demonstrates the cross sections for which the formation of Jupiter stalls at $30\,\mathrm{M}_\oplus$. The dashed contours demonstrate the cross sections for which the formation of Jovian planets near the GC stalls at $10\,\mathrm{M}_\oplus$ (see text for motivation of these conditions). The reflection of light DM candidates implies that the capture efficiency asymptotes. Hence, for a subfraction $f_{\mathrm{DM}} = 10^{-3}$ (shown in chartreuse) there are no constraints below $m_\chi \sim 100$ MeV (the asymptotic value is below the value needed to realise (3)). Finally, in the region below the orange dotted line DM evaporates from the forming planet as discussed in appendix A, given short-range interactions only.

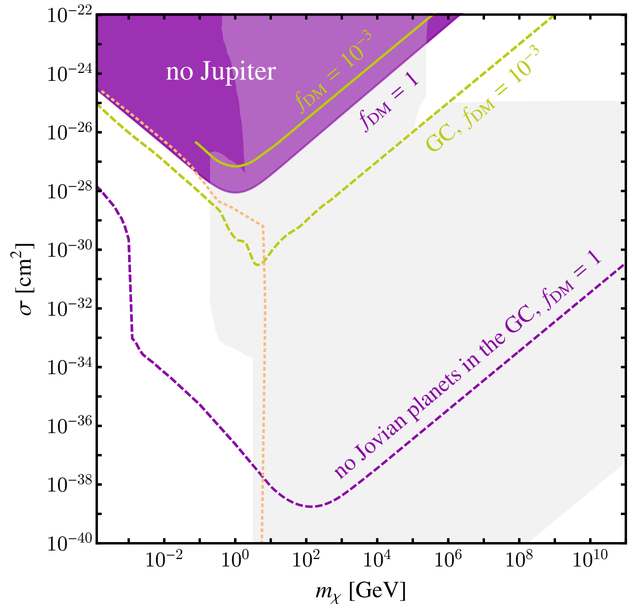

FIG. 3. Constraints on spin-independent DM interactions from the existence of Jupiter, and expected sensitivity from the non-existence of Jovians in the GC, as well as current direct detection constraints– as in Fig.2.

which for DM masses around a GeV, and typical thermal annihilation cross sections is below the Myr time-scale. We therefore assume that the protoplanet reaches annihilation equilibrium, and the total rate of captured DM particles is directly converted to the DM luminosity, as discussed above.

Implications – In Fig. 1 we show the DM fraction needed to halt the formation process for Jupiter in the solar system, using $\rho_{\mathrm{DM}} = 0.42\,\mathrm{GeV\,cm}^{-3}$ and $v_{\mathrm{DM}} = 270\mathrm{km\,s}^{-1}$, we find that f_{cap} increases faster than the fraction necessary to satisfy (3) as a function of time. This does not go on indefinitely, because the rate of gas accumulation rises with increasing mass. Formation studies have shown that after the planet has grown to about $30M_\oplus$ gas capture rises exponentially, however as is seen for the benchmark in Fig. 1 the annihilation of DM captured by the envelope heats the protoplanet enough to halt the formation at about 1.1 Myr, when it is approximately $20\mathrm{M}_\oplus$.

In Figs.2 and 3 we show constraints on the spin-dependent and spin-independent scattering cross sections respectively from the fact that the formation of Jupiter in our solar system has not stopped at a mass of $30\mathrm{M}_\oplus$ as purple contours. For comparison we show current direct detection constraints as gray contours. Here we show the maximal reach in the sensitivity to the direct nuclear recoil process, which are least model dependent. The reach is dominated by the CRESST results at lower masses for spin-independent [96], and spin-dependent [97] cross sections, while at higher masses the LUX [98] results dominate for spin-dependent interactions, while the XENON experiment dominates the spin-independent sensitivity [99]. For large spin-independent cross sections, we also show the XQC constraint [100, 101]. Note that searches based on the Migdal effect [102] could potentially reach lower DM masses, however, the results have large theoretical uncertainties [103], and are not displayed here.

The sensitivity ceiling of direct detection experiments at large cross sections for light DM from Ref. [104] and for heavy DM from Refs. [95, 105] is shown. Since at the large cross sections considered the scaling with atomic mass number is uncertain [94], we do not resale the results for spin-dependent interactions and a more detailed analysis to obtain a precise ceiling values is needed. Note that in contrast the sensitivity of our constraints and suggested search is only affected at cross sections above $10^{-22}\mathrm{cm}^2$, where large drift times would require a more detailed analysis of the DM distribution [28, 106] and annihilation outside the core.

We do not show complementary cosmology-dependent constraints such as those from the CMB and Lymann-α. DM which scatters with a velocity-independent cross-

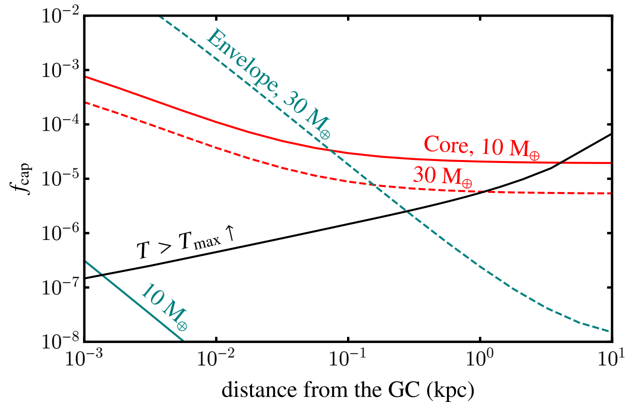

FIG. 4. Benchmark for spin-dependent dark matter: $m_\chi = 5$ GeV, $\sigma_p = 2 \times 10^{-28}\,\mathrm{cm}^2$. The continuous lines show the capture rates at the time when the planet is $10\,\mathrm{M}_\oplus$ and the dashed lines show the rates at $30\,\mathrm{M}_\oplus$.

section can also be constrained from the lack of MW satellites produced in such models [107]. However, as the DM scattering rates could be different in the early universe [108], those bounds are not as universal as the shown late-time sensitivity. Finally, in the case of DM that comprises only a sub-fraction of the total DM abundance, the direct detection constraints are essentially insensitive below the GeV mass scale [109] (and the sensitivity of other constraints also shrinks significantly [110]), while our search covers significant parameter space even at a DM fraction as low as $f_{\rm DM} \sim 10^{-3}$, shown as solid chartreuse lines.

In Figs.2 and 3, we show the sensitivity to DM interactions from observations of Jovians near the GC, for which we have assumed $\rho_{\rm DM} = 100\,\mathrm{GeV\,cm^{-3}}$ and $v_{\rm DM} = 10\,\mathrm{km\,s^{-1}}$, where at small cross sections we find that capture by the core is more efficient than capture by the envelope in both the spin-dependent and the spin-independent case. During the period of formation we are interested in, the core-grow is not appreciable, such that $f_{\rm cap}$ remains approximately constant. As the temperature increase needed to satisfy (2) does grow as a function of time, we expect that formation of Jovian planets in the GC halts at $10\mathrm{M}_\oplus$ in the parameter range indicated by the dashed contours, and proceeds as normal below these contours. Note that the premature ending is already in tension with inferences of Jovian planets in the GC from lensing events [111–113].

In Fig. 4 we show the capture efficiency as a function of distance from the GC assuming an NFW profile and a Maxwellian velocity dispersion. For small DM scattering cross sections, core capture dominates, preventing any gas accumulation for Jovian planets at some distance from the GC. For larger DM cross sections, envelope capture dominates, leading to the formation of Jovian planets with a decreasing mass the closer to the GC they are formed. This distinct phenomenology can be targeted by future observations of exoplanets.

Lastly, as a result of DM heat injection, the protoplanet will respond by radiating away more energy. Even if the heating effect is not significant enough to halt the formation of the gas envelope, this effect leads to an increase in luminosity in high DM-density environments. The luminosity of protoplanet formation peaks in the near-infrared and can be determined by future observations. This allows a direct comparison of the observed peak luminosity, realised at about 2 Myr, and that predicted by theoretical models.

Discussion – In this letter, we have studied the inhibition of the formation of Jupiter in our solar system and Jovian planets in the Milky Way galaxy by the capture and annihilation of DM. We have shown that the heat generated by DM annihilation can increase the temperature of the protoplanet above the temperature at which the gas mixture evaporates, and determined the corresponding constraints on the parameter space of spin-(in)dependent DM. These constraints are competitive for relatively strongly interacting DM candidates, above the "ceiling" of direct detection constraints. We have shown that these constraints are not significantly weakened if only a subfraction of DM is responsible for the heating of protoplanets.

We have also estimated the projected sensitivities from the existence of Jovian planets in the GC, where the DM density is higher and the typical velocity dispersion lower. Future expolanet observations by JWST and Roman may be used to test these scenarios. Moreover, as we explained in the previous section, for a particular DM (sub-component) mass and cross section the formation of Jovian planets is affected as a function of the distance from the GC, enabling a differential detection of the heating signal.

Here we have focused on the core-accretion gas-capture theory of giant planet formation. This is the simplest scenario for the formation of Jovian planets. Alternative scenarios include dynamical processes and migration within the stellar system. Since we focus on the final stages of formation, we expect such alternative scenarios to be qualitatively similar.

ACKNOWLEDGEMENTS

We thank Chris Cappiello, Malcolm Fairbairn, Scott Gaudi, Rebecca Leane, Dave McKeen, and Nirmal Raj for useful conversations and feedback on the manuscript. DC is supported by the STFC under Grant No. ST/T001011/1.

Appendix A: Dark matter evaporation

The condition (3) relies on the fact that hydrogen evaporates for temperatures above $T_{\rm max}$. Therefore, one would naively say that DM candidates with masses below the mass of hydrogen would evaporate at these temperatures too. However, unlike hydrogen, as we demonstrate below the DM particles are concentrated in the core of the objects. Thus, in the short mean free path regime the lower number density of DM particles in the envelope implies a lower flux of escaping particles (2). Here we estimate the evaporation rate of DM particles of a given mass, and compare it to the capture rate.

The DM number density within the protoplanet is obtained by integrating the radial equation Eq. (11) form Ref. [106], under the assumption that the envelope has constant density ρ_E (at t = Myr, $\sim 3\times10^{-8}\mathrm{g\,cm^{-3}}$) and the core has a constant density $\rho_{\rm core}$ (at t = Myr, $\sim 2\mathrm{g\,cm^{-3}}$). We distinguish two regimes, the isothermal regime, where the DM mean free path λ in the object is of the order of the object, and DM thermalises with the core at a constant temperature. The second regime where local thermal equilibrium (LTE) is applicable when the DM mean free path is smaller than the size of the object. Thus we have the total DM profile:

$$n_\chi = \begin{cases} g(r)/N_0 \, \exp\left(-F(r)\right) & \text{if } \lambda < R_E \\ 1/N_0 \exp(-m_\chi \Phi(r)/T(r)) & \text{if } \lambda > R_E \end{cases}, \tag{A1}$$

where the radius is normalised to the envelope size $r = R/R_E$, $\Phi(r)$ is the gravitational potential, $T(r)$ the temperature profile, the normalisation factor N_0 ensured that we have $N_\chi = 4\pi\int_0^{R_E} r^2 n_\chi(r)$, and the LTE functions are given by

$$\frac{F(r)}{\frac{4}{3}\pi G_N m_\chi R_E^2} = \frac{r^2\rho_{\rm core}}{T_{\rm core}}\theta\left(\frac{R_{\rm core}}{R_E}-r\right)+\theta\left(r-\frac{R_{\rm core}}{R_E}\right) \times \frac{\left(1/2\, r^2\rho_E + \left(\frac{R_{\rm core}}{R_E}\right)^3(\rho_{\rm core}-\rho_E)\left(\frac{R_E}{R_{\rm core}}-\frac{1}{r}\right)\right)}{T_E}, \tag{A2}$$

$$g(r) = \theta\left(r-\frac{R_{\rm core}}{R_E}\right)\left(\frac{T_E}{T_{\rm core}}\right)^{\frac{1}{2}\left(\frac{m_\chi}{m_{\rm p}}+1\right)^{-3/2}-1} + \theta\left(\frac{R_{\rm core}}{R_E}-r\right). \tag{A3}$$

For the LTE regime the above equation provides us with the DM density within the last scattering surface, to which we apply the Jeans' escape criterion, demanding that the total surface evaporation rate is below the capture rate. While for the isothermal, and transition regime we use the formalism of Ref. [114, 115] to determine the evaporation mass assuming a core temperature of 3000 K. This leads to the evaporation contour, shown by the dotted lines in Figs. 2, 3. Note that this line is only marking to lowest mass of the DM retained in the object if DM interacts through contact interactions only. In the presence of long range attractive forces, the evaporation contours are significantly moved to lower DM masses, as discussed in Ref. [116].

[1] M. Mayor and D. Queloz, Nature **378**, 355 (1995).
[2] G. Chauvin, A. M. Lagrange, B. Zuckerman, C. Dumas, D. Mouillet, I. Song, J. L. Beuzit, P. Lowrance, and M. S. Bessell, A&A **438**, L29 (2005), arXiv:astro-ph/0504658 [astro-ph].
[3] J. H. C. Martins, N. C. Santos, P. Figueira, J. P. Faria, M. Montalto, I. Boisse, D. Ehrenreich, C. Lovis, M. Mayor, C. Melo, F. Pepe, S. G. Sousa, S. Udry, and D. Cunha, A&A **576**, A134 (2015), arXiv:1504.05962 [astro-ph.EP].
[4] (2020).
[5] J. Brande, T. Barclay, J. E. Schlieder, E. D. Lopez, and E. V. Quintana, The Astronomical Journal **159**, 18 (2019).
[6] S. A. Johnson, M. Penny, B. S. Gaudi, E. Kerins, N. J. Rattenbury, A. C. Robin, S. C. Novati, and C. B. Henderson, The Astronomical Journal **160**, 123 (2020).
[7] M. Benito, F. Iocco, and A. Cuoco, Phys. Dark Univ. **32**, 100826 (2021), arXiv:2009.13523 [astro-ph.GA].
[8] B. Batell, M. Pospelov, A. Ritz, and Y. Shang, Phys. Rev. D **81**, 075004 (2010), arXiv:0910.1567 [hep-ph].
[9] M. Pospelov, A. Ritz, and M. B. Voloshin, Phys. Lett. B **662**, 53 (2008), arXiv:0711.4866 [hep-ph].
[10] M. Pospelov and A. Ritz, Phys. Lett. B **671**, 391 (2009), arXiv:0810.1502 [hep-ph].
[11] I. Z. Rothstein, T. Schwetz, and J. Zupan, JCAP **07**, 018 (2009), arXiv:0903.3116 [astro-ph.HE].
[12] F. Chen, J. M. Cline, and A. R. Frey, Phys. Rev. D **80**, 083516 (2009), arXiv:0907.4746 [hep-ph].
[13] P. Schuster, N. Toro, and I. Yavin, Phys. Rev. D **81**, 016002 (2010), arXiv:0910.1602 [hep-ph].
[14] P. Schuster, N. Toro, N. Weiner, and I. Yavin, Phys. Rev. D **82**, 115012 (2010), arXiv:0910.1839 [hep-ph].
[15] N. F. Bell and K. Petraki, Journal of Cosmology and Astroparticle Physics **2011**, 003–003 (2011).
[16] J. L. Feng, J. Smolinsky, and P. Tanedo, Phys. Rev. D **93**, 015014 (2016), [Erratum: Phys.Rev.D 96, 099901 (2017)], arXiv:1509.07525 [hep-ph].
[17] C. Kouvaris and P. Tinyakov, Phys. Rev. D **82**, 063531 (2010), arXiv:1004.0586 [astro-ph.GA].
[18] J. L. Feng, J. Smolinsky, and P. Tanedo, Phys. Rev. D **93**, 115036 (2016), [Erratum: Phys.Rev.D 96, 099903 (2017)], arXiv:1602.01465 [hep-ph].
[19] R. Allahverdi, Y. Gao, B. Knockel, and S. Shalgar, Phys. Rev. D **95**, 075001 (2017), arXiv:1612.03110 [hep-ph].
[20] R. K. Leane, K. C. Y. Ng, and J. F. Beacom, Phys. Rev. D **95**, 123016 (2017), arXiv:1703.04629 [astro-ph.HE].
[21] C. Arina, M. Backović, J. Heisig, and M. Lucente, Phys. Rev. D **96**, 063010 (2017), arXiv:1703.08087 [astro-ph.HE].
[22] A. Albert *et al.* (HAWC), Phys. Rev. **D98**, 123012

(2018), arXiv:1808.05624 [hep-ph].
[23] A. Albert *et al.* (HAWC), Phys. Rev. D **98**, 123011 (2018), arXiv:1808.05620 [astro-ph.HE].
[24] M. U. Nisa, J. F. Beacom, S. Y. BenZvi, R. K. Leane, T. Linden, K. C. Y. Ng, A. H. G. Peter, and B. Zhou, (2019), arXiv:1903.06349 [astro-ph.HE].
[25] C. Niblaeus, A. Beniwal, and J. Edsjo, JCAP **11**, 011 (2019), arXiv:1903.11363 [astro-ph.HE].
[26] A. Cuoco, P. De La Torre Luque, F. Gargano, M. Gustafsson, F. Loparco, M. Mazziotta, and D. Serini, Phys. Rev. D **101**, 022002 (2020), arXiv:1912.09373 [astro-ph.HE].
[27] D. Serini, F. Loparco, and M. N. Mazziotta (Fermi-LAT), PoS **ICRC2019**, 544 (2020).
[28] J. F. Acevedo, J. Bramante, A. Goodman, J. Kopp, and T. Opferkuch, JCAP **04**, 026 (2021), arXiv:2012.09176 [hep-ph].
[29] M. Mazziotta, F. Loparco, D. Serini, A. Cuoco, P. De La Torre Luque, F. Gargano, and M. Gustafsson, Phys. Rev. D **102**, 022003 (2020), arXiv:2006.04114 [astro-ph.HE].
[30] N. F. Bell, J. B. Dent, and I. W. Sanderson, (2021), arXiv:2103.16794 [hep-ph].
[31] R. K. Leane and T. Linden, (2021), arXiv:2104.02068 [astro-ph.HE].
[32] L. Li and J. Fan, JHEP **10**, 186 (2022), arXiv:2207.13709 [hep-ph].
[33] G. M. French and M. Sher, Phys. Rev. D **106**, 115037 (2022), arXiv:2210.04761 [hep-ph].
[34] A. Ray, Phys. Rev. D **107**, 083012 (2023), arXiv:2301.03625 [hep-ph].
[35] S. Mitra, Phys. Rev. D **70**, 103517 (2004), arXiv:astro-ph/0408341.
[36] R. K. Leane and J. Smirnov, Phys. Rev. Lett. **126**, 161101 (2021), arXiv:2010.00015 [hep-ph].
[37] R. K. Leane, T. Linden, P. Mukhopadhyay, and N. Toro, Phys. Rev. D **103**, 075030 (2021), arXiv:2101.12213 [astro-ph.HE].
[38] R. Garani, N. Raj, and J. Reynoso-Cordova, JCAP **07**, 038 (2023), arXiv:2303.18009 [astro-ph.HE].
[39] I. Goldman and S. Nussinov, Phys. Rev. D **40**, 3221 (1989).
[40] A. Gould, B. T. Draine, R. W. Romani, and S. Nussinov, Phys. Lett. B **238**, 337 (1990).
[41] C. Kouvaris, Phys. Rev. D **77**, 023006 (2008), arXiv:0708.2362 [astro-ph].
[42] G. Bertone and M. Fairbairn, Phys. Rev. D **77**, 043515 (2008), arXiv:0709.1485 [astro-ph].
[43] A. de Lavallaz and M. Fairbairn, Phys. Rev. D **81**, 123521 (2010), arXiv:1004.0629 [astro-ph.GA].
[44] C. Kouvaris and P. Tinyakov, Phys. Rev. D **82**, 063531 (2010), arXiv:1004.0586 [astro-ph.GA].
[45] S. D. McDermott, H.-B. Yu, and K. M. Zurek, Phys. Rev. **D85**, 023519 (2012), arXiv:1103.5472 [hep-ph].
[46] C. Kouvaris and P. Tinyakov, Phys. Rev. Lett. **107**, 091301 (2011), arXiv:1104.0382 [astro-ph.CO].
[47] T. Guver, A. E. Erkoca, M. Hall Reno, and I. Sarcevic, JCAP **1405**, 013 (2014), arXiv:1201.2400 [hep-ph].
[48] J. Bramante, K. Fukushima, and J. Kumar, Phys. Rev. **D87**, 055012 (2013), arXiv:1301.0036 [hep-ph].
[49] N. F. Bell, A. Melatos, and K. Petraki, Phys. Rev. **D87**, 123507 (2013), arXiv:1301.6811 [hep-ph].
[50] J. Bramante, K. Fukushima, J. Kumar, and E. Stopnitzky, Phys. Rev. **D89**, 015010 (2014), arXiv:1310.3509 [hep-ph].
[51] B. Bertoni, A. E. Nelson, and S. Reddy, Phys. Rev. D **88**, 123505 (2013), arXiv:1309.1721 [hep-ph].
[52] C. Kouvaris and P. Tinyakov, Phys. Rev. **D83**, 083512 (2011), arXiv:1012.2039 [astro-ph.HE].
[53] M. McCullough and M. Fairbairn, Phys. Rev. D **81**, 083520 (2010), arXiv:1001.2737 [hep-ph].
[54] M. Angeles Perez-Garcia and J. Silk, Phys. Lett. **B744**, 13 (2015), arXiv:1403.6111 [astro-ph.SR].
[55] J. Bramante, Phys. Rev. Lett. **115**, 141301 (2015), arXiv:1505.07464 [hep-ph].
[56] P. W. Graham, S. Rajendran, and J. Varela, Phys. Rev. **D92**, 063007 (2015), arXiv:1505.04444 [hep-ph].
[57] M. Cermeno, M. Perez-Garcia, and J. Silk, Phys. Rev. **D94**, 063001 (2016), arXiv:1607.06815 [astro-ph.HE].
[58] P. W. Graham, R. Janish, V. Narayan, S. Rajendran, and P. Riggins, Phys. Rev. **D98**, 115027 (2018), arXiv:1805.07381 [hep-ph].
[59] J. F. Acevedo and J. Bramante, Phys. Rev. **D100**, 043020 (2019), arXiv:1904.11993 [hep-ph].
[60] R. Janish, V. Narayan, and P. Riggins, Phys. Rev. **D100**, 035008 (2019), arXiv:1905.00395 [hep-ph].
[61] R. Krall and M. Reece, Chin. Phys. **C42**, 043105 (2018), arXiv:1705.04843 [hep-ph].
[62] M. Baryakhtar, J. Bramante, S. W. Li, T. Linden, and N. Raj, Phys. Rev. Lett. **119**, 131801 (2017), arXiv:1704.01577 [hep-ph].
[63] N. Raj, P. Tanedo, and H.-B. Yu, Phys. Rev. **D97**, 043006 (2018), arXiv:1707.09442 [hep-ph].
[64] N. F. Bell, G. Busoni, and S. Robles, JCAP **1809**, 018 (2018), arXiv:1807.02840 [hep-ph].
[65] C.-S. Chen and Y.-H. Lin, JHEP **08**, 069 (2018), arXiv:1804.03409 [hep-ph].
[66] B. Dasgupta, A. Gupta, and A. Ray, JCAP **08**, 018 (2019), arXiv:1906.04204 [hep-ph].
[67] K. Hamaguchi, N. Nagata, and K. Yanagi, Phys. Lett. **B795**, 484 (2019), arXiv:1905.02991 [hep-ph].
[68] D. A. Camargo, F. S. Queiroz, and R. Sturani, JCAP **1909**, 051 (2019), arXiv:1901.05474 [hep-ph].
[69] N. F. Bell, G. Busoni, and S. Robles, JCAP **1906**, 054 (2019), arXiv:1904.09803 [hep-ph].
[70] J. F. Acevedo, J. Bramante, R. K. Leane, and N. Raj, JCAP **03**, 038 (2020), arXiv:1911.06334 [hep-ph].
[71] A. Joglekar, N. Raj, P. Tanedo, and H.-B. Yu, (2019), arXiv:1911.13293 [hep-ph].
[72] A. Joglekar, N. Raj, P. Tanedo, and H.-B. Yu, (2020), arXiv:2004.09539 [hep-ph].
[73] N. F. Bell, G. Busoni, S. Robles, and M. Virgato, (2020), arXiv:2004.14888 [hep-ph].
[74] R. Garani, A. Gupta, and N. Raj, (2020), arXiv:2009.10728 [hep-ph].
[75] J. Bramante, B. J. Kavanagh, and N. Raj, Phys. Rev. Lett. **128**, 231801 (2022), arXiv:2109.04582 [hep-ph].
[76] J. Coffey, D. McKeen, D. E. Morrissey, and N. Raj, Phys. Rev. D **106**, 115019 (2022), arXiv:2207.02221 [hep-ph].
[77] K. Freese, P. Gondolo, J. A. Sellwood, and D. Spolyar, Astrophys. J. **693**, 1563 (2009), arXiv:0805.3540 [astro-ph].
[78] M. Taoso, G. Bertone, G. Meynet, and S. Ekstrom, Phys. Rev. D **78**, 123510 (2008), arXiv:0806.2681 [astro-ph].
[79] C. Ilie, C. Levy, J. Pilawa, and S. Zhang, (2020), arXiv:2009.11478 [astro-ph.CO].

[80] C. Ilie, C. Levy, J. Pilawa, and S. Zhang, (2020), arXiv:2009.11474 [astro-ph.CO].
[81] J. Lopes and I. Lopes, Astron. Astrophys. **651**, A101 (2021), arXiv:2107.13885 [astro-ph.SR].
[82] S. A. R. Ellis, (2021), arXiv:2111.02414 [astro-ph.CO].
[83] D. Croon and J. Sakstein, (2023), arXiv:2309.XXXXX [hep-ph].
[84] J. Bramante, J. Kumar, G. Mohlabeng, N. Raj, and N. Song, (2022), arXiv:2210.01812 [hep-ph].
[85] J. Bramante and N. Raj, (2023), arXiv:2307.14435 [hep-ph].
[86] O. Hubickyj, P. Bodenheimer, and J. J. Lissauer, Icarus **179**, 415 (2005).
[87] F. Adams and K. Batygin, in *AAS/Division for Planetary Sciences Meeting Abstracts*, AAS/Division for Planetary Sciences Meeting Abstracts, Vol. 54 (2022) p. 102.02.
[88] G. D'Angelo, S. J. Weidenschilling, J. J. Lissauer, and P. Bodenheimer, Icarus **355**, 114087 (2021), arXiv:2009.05575 [astro-ph.EP].
[89] J. Jeans, *The Dynamical Theory of Gases*, 4th ed., Cambridge Library Collection - Physical Sciences (Cambridge University Press, 2009).
[90] J. J. Lissauer, O. Hubickyj, G. D'Angelo, and P. Bodenheimer, Icarus **199**, 338 (2009), arXiv:0810.5186 [astro-ph].
[91] G. D'Angelo, S. J. Weidenschilling, J. J. Lissauer, and P. Bodenheimer, Icarus **355**, 114087 (2021).
[92] R. Leane and J. Smirnov, (2023), arXiv:2308.XXXXX [hep-ph].
[93] R. K. Leane and J. Smirnov, "Asteria: A Package for Dark Matter Capture in Celestial Objects," `https://zenodo.org/record/8150110` (2023).
[94] M. C. Digman, C. V. Cappiello, J. F. Beacom, C. M. Hirata, and A. H. G. Peter, Phys. Rev. D **100**, 063013 (2019), arXiv:1907.10618 [hep-ph].
[95] C. V. Cappiello, J. I. Collar, and J. F. Beacom, Phys. Rev. D **103**, 023019 (2021), arXiv:2008.10646 [hep-ex].
[96] G. Angloher *et al.* (CRESST), Phys. Rev. D **107**, 122003 (2023), arXiv:2212.12513 [astro-ph.CO].
[97] G. Angloher *et al.* (CRESST), Phys. Rev. D **106**, 092008 (2022), arXiv:2207.07640 [astro-ph.CO].
[98] D. S. Akerib *et al.* (LUX), Phys. Rev. Lett. **118**, 251302 (2017), arXiv:1705.03380 [astro-ph.CO].
[99] E. Aprile *et al.* ((XENON Collaboration)††, XENON), Phys. Rev. Lett. **131**, 041003 (2023), arXiv:2303.14729 [hep-ex].
[100] A. L. Erickcek, P. J. Steinhardt, D. McCammon, and P. C. McGuire, Phys. Rev. **D76**, 042007 (2007), arXiv:0704.0794 [astro-ph].
[101] M. S. Mahdawi and G. R. Farrar, JCAP **10**, 007 (2018), arXiv:1804.03073 [hep-ph].
[102] Z. Y. Zhang *et al.* (CDEX), Phys. Rev. Lett. **129**, 221301 (2022), arXiv:2206.04128 [hep-ex].
[103] P. Cox, M. J. Dolan, C. McCabe, and H. M. Quiney, Phys. Rev. D **107**, 035032 (2023), arXiv:2208.12222 [hep-ph].
[104] C. V. Cappiello, Phys. Rev. Lett. **130**, 221001 (2023), arXiv:2301.07728 [hep-ph].
[105] B. J. Kavanagh, Phys. Rev. D **97**, 123013 (2018), arXiv:1712.04901 [hep-ph].
[106] R. K. Leane and J. Smirnov, (2022), arXiv:2209.09834 [hep-ph].
[107] E. O. Nadler, V. Gluscevic, K. K. Boddy, and R. H. Wechsler, Astrophys. J. Lett. **878**, 32 (2019), [Erratum: Astrophys.J.Lett. 897, L46 (2020), Erratum: Astrophys.J. 897, L46 (2020)], arXiv:1904.10000 [astro-ph.CO].
[108] G. Elor, R. McGehee, and A. Pierce, Phys. Rev. Lett. **130**, 031803 (2023), arXiv:2112.03920 [hep-ph].
[109] D. McKeen, M. Moore, D. E. Morrissey, M. Pospelov, and H. Ramani, (2022), arXiv:2202.08840 [hep-ph].
[110] Y. Li, Z. Liu, and Y. Xue, JCAP **05**, 060 (2023), arXiv:2209.04387 [hep-ph].
[111] K. C. Sahu *et al.*, Nature **443**, 534 (2006), arXiv:astro-ph/0610098.
[112] J. Janczak *et al.* (MOA, muFUN, MiNDSTEp Consortium, PLANET), Astrophys. J. **711**, 731 (2010), arXiv:0908.0529 [astro-ph.EP].
[113] N. Koshimoto, D. P. Bennett, D. Suzuki, and I. A. Bond, The Astrophysical Journal Letters **918**, L8 (2021).
[114] A. Gould, ApJ **321**, 560 (1987).
[115] A. Gould, ApJ **356**, 302 (1990).
[116] J. F. Acevedo, R. K. Leane, and J. Smirnov, (2023), arXiv:2303.01516 [hep-ph].